Large deformation and stress analysis of isotropic annular membranes by differential quadrature method [†]

A. A. Atai[*] and M. Mozaffari

Department of Mechanical Engineering, Islamic Azad University, Karaj Branch, Karaj, Iran

---

Abstract

In this paper, the differential quadrature method (DQM) was employed to study nonlinear analysis of annular isotropic membrane in which an attempt was made to explore the applicability and accuracy of DQM for nonlinear analysis of a structural membrane. For this purpose, the large deformation analyses of symmetric circular membranes were investigated. Relaxed strain energy function in conjunction with Green's strain and perfectly flexible assumptions was utilized for modeling the nonlinear behavior of the membranes. The nonlinear governing equations were discretized at whole domain grid points, and boundary conditions were implemented exactly at boundary grid points. Comparative studies were made between approaches for different boundaries. Convergence of the methodology was demonstrated, and the results were compared with existing solutions of other methods, such as dynamic relaxation. It was shown that accurate results were obtained even when utilizing only a small number of grid points.

Keywords: Membrane; Annular; Isotropic; Large deformation; Differential quadrature method (DQM)

---

1. Introduction

Membrane structures have long been under consideration as structural elements because of advantages such as high strength to weight ratio and low cost. In exterior wall systems and roofing systems, the term membrane is widely utilized to refer to a relatively thin, usually flexible layer of material within or at the surface of a building enclosure system.

The theory of mechanics and performance of the tensile structure is well established by Otto [1] and many others. Deformation and stress analysis of these particular structures are associated with solving the nonlinear behavior of structures that originated from the large deformation and nonlinear responses of materials. There are various choices to analyze and solve membrane equations. One of the most significant methods is dynamic relaxation, which was utilized by Atai and Steigmann [2] and Haseganu and Steigmann [3]. In this methodology, the different forms of the equations of equilibrium are derived using Green's theorem, and dynamic relaxation (which considers the problem as a damped dynamic one) is applied to solve the equations. Much research work has been published on developing an appropriate wind testing protocol for the single-ply membrane roof system [4-6].

The commonly used numerical methods in structural mechanics analysis are the finite element method, finite difference method, boundary element method, and Rayleigh-Ritz method. As an efficient alternative numerical tool, differential quadrature methods (DQMs) have been used for structural analysis. Details on the development and applications may be found in the review paper by Bert and Malik [7]. Among the different approaches for determining the weighting coefficients [7], Lagrange interpolation functions and trigonometric/harmonic functions are the most popular test functions. The applications of polynomial differential quadrature (PDQ) for thin beams and plates and also for rectangular thick plates were carried out by Malekzadeh [8]. Liew and Han [9] employed the DQ method to present the bending analysis of simply supported thick skew plates based on the first-order shear deformation plate theory.

In this paper, the capabilities of DQ methods for deformation analysis of flexible membranes' deformation in three dimensions are investigated. There is clearly a need to study a new speedy accurate methodology on membrane structures with a small number of grid points. This paper applies theory of elastics to membrane and discretizes the resulting equations in the axial direction by DQM and, for the solution procedure, develops a theory to model the membrane structures in various boundary conditions.

---

2. Mechanical characteristics of the three-dimensional flexible membrane

2.1 Continuum mechanics

In this section, we discuss the analysis of perfectly flexible elastic surfaces, so we consider the reference configuration to be flat and stress-free. In addition, we assume that the reference configuration occupies a bounded region Ω in the (x_1, x_2) plane with piecewise smooth boundary $\partial\Omega$. Each point of the membrane in this configuration is identified by its position vector $X = x_\alpha e_\alpha$, where the Greek indices range over $\{1, 2\}$ and $\{e_1, e_2\}$ is a fixed orthonormal basis that spans Ω.

A general three-dimensional (3D) deformation maps the position vector X to the deformed position vector $y(X) = y_i(X)e_i$, where the Latin indices range over $\{1, 2, 3\}$ and $e_3 = e_1 \times e_2$. The deformation gradient F, which maps the element dX in the reference plane onto $dy(X) = FdX$ tangent to the deformed surface, can be expressed by

$$F(X) = grad(X) = F_{i\alpha}(X)e_i \otimes e_\alpha. \tag{1}$$

Then as in convectional continuum mechanics, the associated Cauchy-Green strain tensor is

$$C = F^T F = C_{\alpha\beta} e_\alpha \otimes e_\beta. \tag{2}$$

It can be easily seen that C is a positive semidefinite tensor and, therefore, it can be represented in the following spectral form:

$$C = \lambda_1^2 u_1 \otimes u_1 + \lambda_2^2 u_2 \otimes u_2, \tag{3}$$

where u_1 and u_2 are the orthonormal principal vectors of strain and $\lambda_\alpha = |Fu_\alpha| = (u_\alpha.Cu_\alpha)^{1/2}$. These can be used to define the unit vectors:

$$U_\alpha = \lambda_\alpha^{-1} Fu_\alpha, \alpha = 1, 2. \tag{4}$$

The Cauchy-Green strain tensor is

$$\begin{aligned} C = \lambda_1^2 u_1 \otimes u_1 + \lambda_2^2 u_2 \otimes u_2 \\ + \lambda_1\lambda_2 U_1.U_2(u_1 \otimes u_2 + u_2 \otimes u_1) \end{aligned}. \tag{5}$$

As in the elastic curve, we assume the existence of a strain energy W, per unit area Ω, that responds only to changes in the local intrinsic or metric geometry of the surface. This formulates the intuitive notion of a perfectly flexible membrane. Thus, we assume that

$$W(F) = \hat{W}(F^T F) = \hat{W}(C). \tag{6}$$

It can be easily seen that W is invariant under a superimposed rigid motion. Non-uniform elastic properties may be taken into account by letting W depend explicitly on X.

The surface analog of the second Piola-Kirchhoff stress is

$$S = S_{\alpha\beta} e_\alpha \otimes e_\beta; \quad S_{\alpha\beta} = \frac{\partial\hat{W}}{\partial C_{\alpha\beta}} + \frac{\partial\hat{W}}{\partial C_{\beta\alpha}}. \tag{7}$$

The Piola stress is

$$T = F.S = T_{i\alpha} e_i \otimes e_\alpha. \tag{8}$$

If the surface is in equilibrium under applied or reactive edge forces, and the distributed forces are negligible, then the Piola stress must satisfy

$$divT = 0 \quad in\ \Omega \tag{9}$$

For isotropic materials, the strain energy is expressible as a symmetric function of the principal stretches:

$$W(F) = \hat{W}(C) = w(\lambda_1, \lambda_2). \tag{10}$$

Then the Piola stress can be calculated from

$$T = w_1 U_1 \otimes u_1 + w_2 U_2 \otimes u_2, \tag{11}$$

where

$$w_\alpha = \partial w / \partial\lambda_\alpha. \tag{12}$$

2.2 Relaxation theory

Although it seems the calculation ended by satisfying the Piola stress in the equilibrium equation, because of the fact that the membrane cannot withstand in-plane compressive loading, we utilized relaxed strain energy, which is described as

$$w_R(\lambda_1, \lambda_2) = w(\lambda_1, \lambda_2) \quad if \tag{13}$$
$$\lambda_1 \geq \nu(\lambda_2), \lambda_2 \geq \nu(\lambda_1),$$
$$w_R(\lambda_1, \lambda_2) = \hat{w}(\lambda_1) \quad if \tag{14}$$
$$\lambda_1 \geq 1, \lambda_2 \leq \nu(\lambda_1),$$
$$w_R(\lambda_1, \lambda_2) = \hat{w}(\lambda_2) \quad if \tag{15}$$
$$\lambda_2 \geq 1, \lambda_2 \leq \nu(\lambda_1) \quad and$$
$$w_R(\lambda_1, \lambda_2) = 0 \quad if \tag{16}$$
$$\lambda_1 \leq 1, \lambda_2 \leq 1.$$

$\nu(x)$ is a solution of

$$w_2(x, \nu(x)) = w_1(\nu(x), x) = 0 \tag{17}$$

and called the *natural width in simple tension*.

In this study, we used several membrane strain energy function whose relaxation meets the foregoing conditions. Each of these involves a material constant μ with dimensions of force/length (or energy/area).

As mentioned above, the relaxation of the Neo-Hookian [10] strain energy is defined by

$$w\,(\lambda_1,\lambda_2) = 1/2\mu(\lambda_1^2 + \lambda_2^2 + 1/\lambda_1^2\lambda_1^2 - 3), \tag{18}$$

$$\hat{w}(x) = 1/2\mu(x^2 + 2x^{-1} - 3), v(x) = x^{-1/2}. \tag{19}$$

The relaxed form of the Varga [11] strain energy is given by

$$w\,(\lambda_1,\lambda_2) = 2\mu(\lambda_1 + \lambda_2 + 1/\lambda_1\lambda_2 - 3), \tag{20}$$

$$\hat{w}(x) = 2\mu(x + 2x^{-1/2} - 3), v(x) = x^{-1/2}. \tag{21}$$

3. Review of the differential quadrature method

The method of differential quadrature is based on the idea that the partial derivative of a field variable at the *i*th discrete point in the computational domain is approximated by a weighted linear sum of the values of the field variable along the line that passes through that point, which is parallel with the coordinate direction of the derivative [7]. Consider a two-dimensional field variable $u\,(x,\,y)$. Its *m*th-order derivative with respect to *x*, and its (*m*+*n*)th order derivative with respect to *x* and *y* are approximated as

$$\left.\frac{\partial^m u}{\partial x^m}\right|_{(x_i,y_j)} = \sum_{k=1}^{N_x} \overline{A}_{ik}^{(m)} u(x_k, y_j), \tag{22}$$

$$\left.\frac{\partial^{m+n} u}{\partial x^m \partial y^n}\right|_{(x_i,y_j)} = \sum_{k=1}^{N_x} \overline{A}_{ik}^{(m)} \overline{A}_{jl}^{(n)} u(x_k, y_l) \tag{23}$$

There are two key points in the successful application of the DQM. One is how to determine the weighting coefficients, and the other is how to select the grid points. The method developed by Shu and Richard [7] is claimed to be computationally more accurate than other methods. According to the Shu and Richard rule, the weighting coefficients of the first-order derivatives in the ξ direction ($\xi = x$ or y) are determined as

$$\overline{A}_{ij}^{(1)} = \begin{cases} \dfrac{M(\xi_i)}{(\xi_i - \xi_j)M(\xi_j)} & for\ \ i \neq j \\[2ex] -\displaystyle\sum_{j=1,i\neq j}^{N_\xi} \overline{A}_{ij}^{(1)} & for\ \ i = j \end{cases}, \tag{24}$$

where

$$M(\xi_i) = \prod_{j=1,i\neq j}^{N_\xi} (\xi_i - \xi_j) \tag{25}$$

It was demonstrated that non-uniform grid points give a better result with the same number of equally spaced grid points [7]. In this paper, we chose this set of grid points in terms of natural coordinate directions *x* and *y* as

$$\xi_i = \frac{1}{2}\left[1 - \cos\left[\frac{(i-1)\pi}{(N_\xi - 1)}\right]\right]. \tag{26}$$

4. Numerical results

Although the governing equations for the membrane could be written in terms of $y(x)$ and its derivatives, the resulting equations will be highly complicated and second- and higher-order derivatives must also be formulated using DQM and incorporated into the equations. Also, some parameters of interest, such as principal stretches and stresses, must be later computed from $y(x)$ and its derivatives in the post-processing phase. To avoid these, the following parameters are treated as unknown in the procedure: $\mathbf{y(x)}$, principal directions U_α and u_α, stretches, and components of the Piola stress $\boldsymbol{T}$. In this way, the governing equations remain as first-order differentials, and it will be also easier to apply boundary conditions.

By discretizing all equations in each grid point, we achieve the following equations:

$$\sum_{m=1}^{N_{x_1}} A^{x_1}{}_{im} T^{11}{}_{mj} + \sum_{n=1}^{N_{x_2}} A^{x_2}{}_{jn} T^{12}{}_{in} = 0, \tag{27}$$

$$\sum_{m=1}^{N_{x_1}} A^{x_1}{}_{im} T^{21}{}_{mj} + \sum_{n=1}^{N_{x_2}} A^{x_2}{}_{jn} T^{22}{}_{in} = 0, \tag{28}$$

$$\sum_{m=1}^{N_{x_1}} A^{x_1}{}_{im} T^{31}{}_{mj} + \sum_{n=1}^{N_{x_2}} A^{x_2}{}_{jn} T^{32}{}_{in} = 0. \tag{29}$$

4.1 Example 1

In this section, we try to calculate plane deformation. A Varga annular membrane bounded by concentric circles is considered first. Fig. 1 shows the meshed initial configuration used for the computation. The ratio of the radii of the internal and external circular boundaries was taken to be 0.5. Without imposing any symmetry on the free nodes, the outer boundary was displaced radially as specified below:
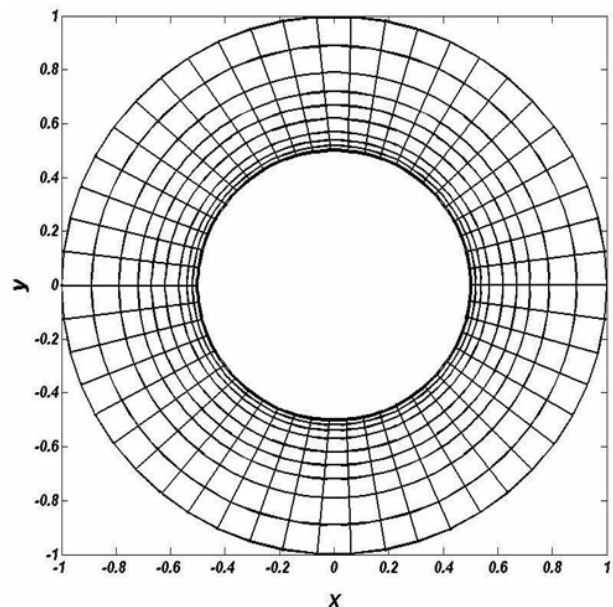

Fig. 1. Meshed reference configuration of an annular membrane.

$$r_i / r_o = 0.5, \quad \rho_0 / r_o = 1.2 . \tag{30}$$

r is the undeformed radius, and ρ is the corresponding deformed radius at each point in the membrane, and indices i and o refer to the inner and outer boundaries, respectively. The boundary condition for this situation can be expressed in discretized form as below (for nodes on external circular boundary):

$$\rho_{0_i} = 1.2 \times r_{o_i} . \tag{31}$$

For traction-free inner boundaries:

$$T.N = 0 . \tag{32}$$

N is the outward unit normal to the boundaries.

The deformed configuration of the mesh is represented with continuous lines in Fig. 2. The credibility of the solution procedures for large deformations and stress analysis of isotropic annular membranes were further examined by comparing the solutions with those of exact solutions obtained by analytical equations for Varga annular membranes, which is explained below.

By assuming biaxial tension everywhere in the membrane and based on the stretches belonging to the first branch of the relaxed Varga strain energy, the equilibrium equation reduces to:

$$-4\mu J^{-3} FgradJ = 0 , \tag{33}$$

where

$$J = \frac{\rho \rho'}{r} = Const. \tag{34}$$

Applying this to the boundary condition yields

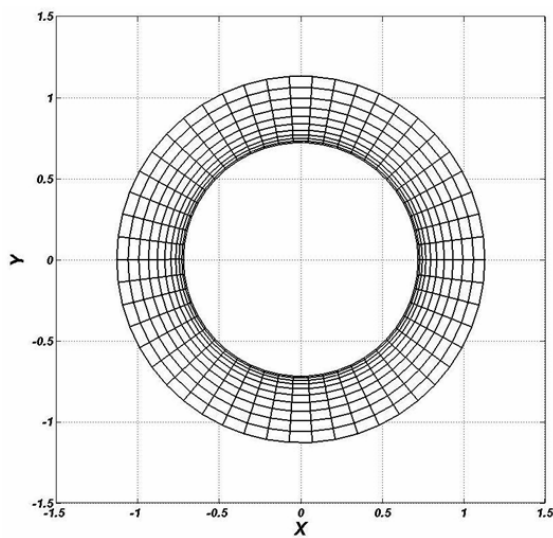$$\rho(r) = [\rho_0^2 - J(r_o^2 - r^2)]^{0.5} . \tag{35}$$

Fig. 2. Deformed configuration.

We use the coupling condition to calculate J:

$$f(\lambda_2(r_i))/r_i = 2\mu(1 - \lambda_2(r_i)/J^2) . \tag{36}$$

However from Eq. (35):

$$\lambda_2(r_i) = \frac{\rho(r_i)}{r_i} = \left\{ (\frac{\rho_0}{r_i})^2 - J[(\frac{r_o}{r_i})^2 - 1] \right\}^{0.5} . \tag{37}$$

Therefore we will have

$$\lambda_1(r_i) = \frac{\partial \rho(r_i)}{\partial r} . \tag{38}$$

Fig. 3 shows the comparison of distribution of analytical and numerical radial and hoop stretches versus radius for the particular case that consists of 11 Chebyshev-Gauss-Lobatto divisions radially and 50 equally spaced divisions circumferentially. The solid curves show the analytical results, while the squares show the numerical values for the hoop and radial stretch. From the results presented in Fig. 3, an excellent agreement can be seen between the solutions of the present method and that of the other analytical method.
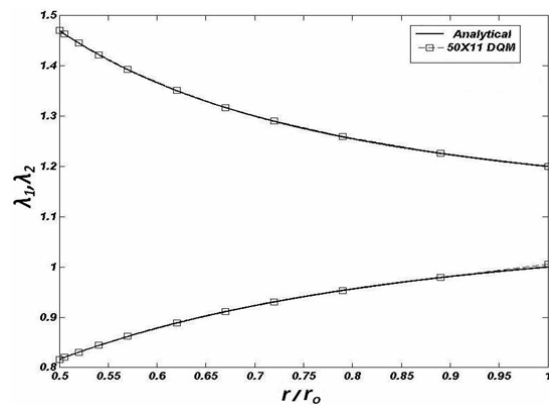

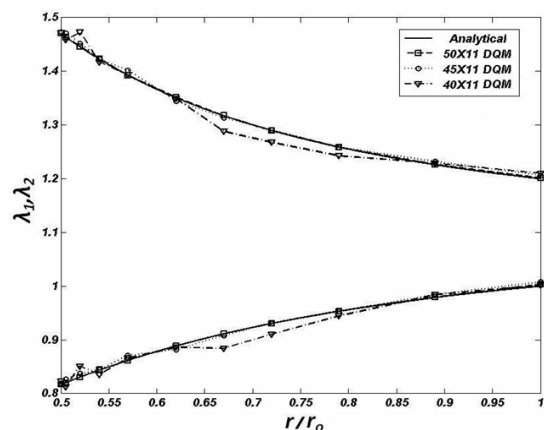Fig. 3. The comparison of distribution of analytical and numerical stretches (50×11).

Fig. 4. The comparison of distribution of analytical and numerical stretches in different meshes.

The effects of the different values of the radial and circular meshes on the convergence and accuracy for annular membranes are presented in Fig. 4, in which radial and circular meshes that trigger high accuracy solutions are shown.

Additionally, the preference of the solution procedures for large deformation analysis of annular membranes was further examined by comparing the solutions with those of other numerical solution, such as Dynamic Relaxation (DR) obtained by Atai [2]. Excellent agreement of the two approaches, i.e., DQM and DRM with analytical approach, and less computational effort of the present DQM (50×11) with respect to DRM (72×11: +30%) depict the efficiency of the present DQM as a methodology for nonlinear analysis of annular membrane (Fig. 5).
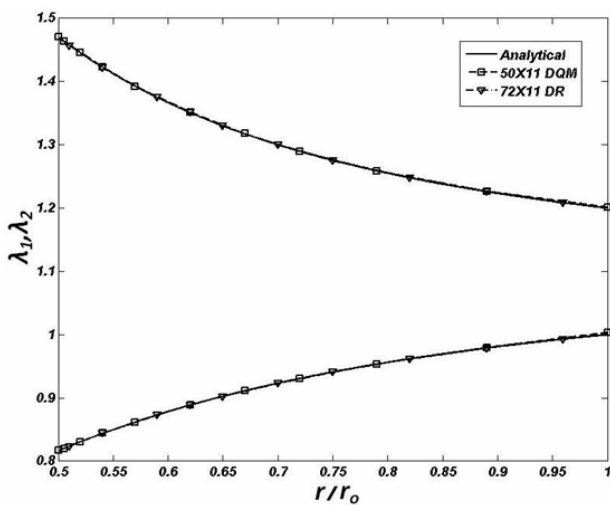

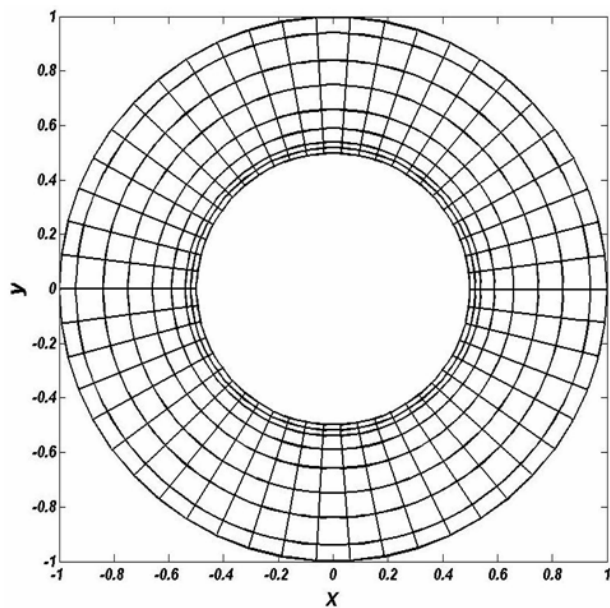Fig. 5. The comparison stretches between DQM (50×11) and DR (72×11).

Fig. 6. Meshed reference configuration of an annular membrane.

4.2 Example 2

In this section, we try to calculate combined twist and lateral deflection in a Neo-Hookean membrane. A circular annular membrane with a 0.5 ratio of radii of the internal and external boundaries and with meshed reference configuration as in Fig. 6 was considered. Holding the external boundary fixed, the ratio of the radii was reduced to 0.25. The boundary condition for this situation can be expressed in discretized form as below (for nodes on the inner circular boundary):

$$\rho_{0_i} = 0.25 . \tag{39}$$

This intermediate deformed configuration is represented in Fig. 7. Wrinkling occurred in a zone immediately adjacent to the inner boundary. The radial tension trajectories indicate the extent of the wrinkled region. Next, the inner boundary was displaced vertically by an amount equal to the radius of the external boundary. As can be seen in Fig. 8, the extent of the wrinkled region decreased. This is followed by a 90° counterclockwise rotation of the inner boundary. The deformed configuration of the mesh is shown in Figs. 9 and 10. The mem-
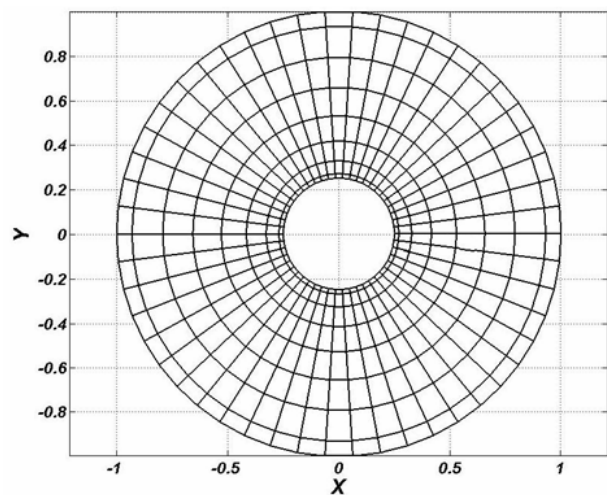

Fig. 7. First stage: Radial displacement, and reduction in circumference of the inner boundary of the circular membrane.
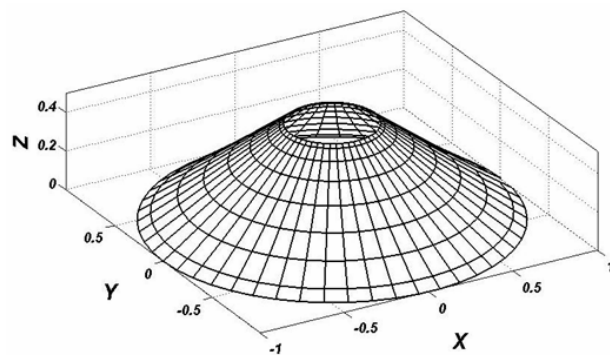

Fig. 8. Second stage: Combined radial displacement and lateral deflection of the circular membrane.

Table 1. Comparison of λ_{MAX} in different deformation stages.

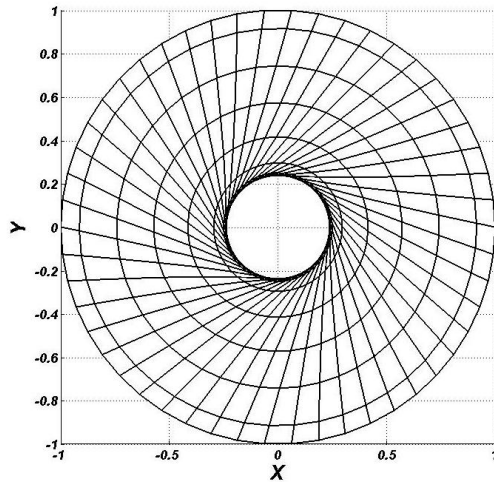| Deformation Stage	λ_{MAX}	
	Haseganu [3] 72×11	DQM 9×50 (−43%)
Stage 1	1.82	1.8282
Stage 2	3.39	3.3912
Stage 3	3.98	3.9865

Fig. 9. Third stage: Combined radial displacement, lateral deflection, and twist of the circular annular membrane.
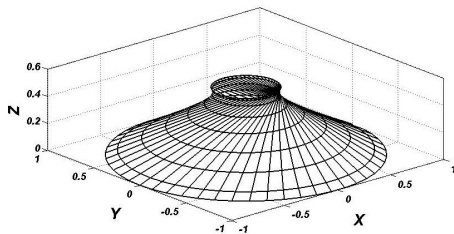

Fig. 10. Third stage: Combined radial displacement, lateral deflection, and twist of the circular membrane.

brane was tense elsewhere. The extent of wrinkling increased with the increase in rotation angle and dimensioned with increasing lateral displacement. This behavior is in qualitative agreement with the analysis of Roxburg and Steigmann, in which axisymmetry was assumed at the outset, and a more refined strain energy function was used.

The maximum principal stretch computed increased from 1.8282 in the solution represented in Fig. 7 to 3.3912 for the solution in Fig. 8 and finally to 3.9865 for the solution in Fig. 10. It occurred in all three cases on the circle of the inner boundary. The last two values are outside the range for which the Neo-Hookean material furnishes quantitative agreement with experimental data on rubber. Finally, this methodology and the dynamic relaxation method released by Haseganu are compared in Table 1, in which one can see the excellent rate of convergence and accuracy.

5. Conclusion

The applicability and efficiency of the DQM was investigated for nonlinear structural analysis by considering the large deformation analysis of annular isotropic membranes. An excellent rate of convergence was demonstrated, and the results are in good agreement with the solutions of other methods even with a few number of grid points in all examples presented.

In the numerical examples, the effects of plane deformation and combined twist and lateral deflection on the nonlinear behavior of annular membranes under different boundary conditions were studied. Excellent agreement of the DQ approach and less computational effort of the present DQM with respect to the dynamic relaxation method depict the efficiency of the present DQM for nonlinear analysis of isotropic membranes. This methodology can be used as an efficient numerical tool for the solution of nonlinear structural membrane problems.

References

[1] F. Otto, *Tensile structures*. The MIT Press; (1973).

[2] A. A. Atai and D. J. Steigmann, Coupled Deformation of elastic curves and surfaces. *International Journal of Solids and Structures*, (35) (1998) 1915-1952.

[3] E. Haseganu and D. J. Steigmann, Equilibrium analysis of finitely deformed elastic networks. *Computational Mechanics* (17) (1996) 359-373.

[4] N. J. Cook, Dynamic responses of single-ply membrane roofing systems, *Journal of Wind Engineering and Industrial Aerodynamics,* 41-44 (1992) 1525-1536.

[5] M. Mozaffari, A. A. Atai and N. Mostafa, Large deformation and mechanics of flexible isotropic membrane ballooning in three dimensions by differential quadrature method, *Journal of Mechanical Science and Techonology* (23) (2009) 2921-2927.

[6] A. Baskaran, Y. Chen and M. G. Savage, Development of a wind load cycle for testing commercial building envelopes. *ASCE Structures Congress XV*, Portland, Oregon, USA., (1997) 25-32.

[7] C. W. Bert and M. Malik Differential Quadrature Method in computational mechanics: A review. *Applied Mechanics Review,* 49 (1996) 1-27.

[8] G. Karami and P. Malekzadeh A new differential quadrature methodology for beam analysis and the associated DQEM. *Computer Methods in Applied Mechanics and Engineering,* 191 (2002) 3509-3026.

[9] K. M. Liew and J. B. Han. A four-node differential quadrature method for straight-sided quadrilateral Reissner/Mindlin plates. *Communication in Numerical Methods in Engineering,* 13 (1997) 73-81.

[10] Pipkin, The relaxed energy density for isotropic elastic membranes, *IMA Journal of Applied Mathematics* (36) (1986) 85-99.

[11] Varga, *Stress Strain Behavior of Elastic Materials*. Wiley, New York, (1966).

Ali Asghar Atai received his B.Sc. in Mechanical Engineering from the University of Tehran, Iran, in 1990. He obtained his M.Sc. and Ph.D. from the University of Alberta, Canada, in 1994 and 1998, respectively. He is currently a professor at the Department of Mechanical Engineering, Islamic Azad University, Karaj Branch, Iran. His areas of research interest include flexible structural mechanics, continuous media, and dynamics of machines.